Zero valent sulfur is the product of assimilatory sulfite reductase and a substrate of cysteine synthase

Qun Cao,[1,2,3,†] Xuanyu Liu,[1,†] Xi Zhang,[1,4] Qingda Wang,[1] Yongzhen Xia,[1] Luying Xun,[1,5] Huaiwei Liu[1,*]

[1]State Key Laboratory of Microbial Technology, Shandong University, Qingdao, 266200, People's Re-public of China.

[2]Department of Neurosurgery, Qilu Hospital, Cheeloo College of Medicine and Institute of Brain and Brain-Inspired Science, Shandong University, Jinan, 250012, China

[3]Jinan Microecological Biomedicine Shandong Laboratory and Shandong Key Laboratory of Brain Health and Function Remodeling, Jinan, 250017, China

[4]Institute of Medical Sciences, the Second Hospital of Shandong University, Jinan, 250033, PR China

[5]School of Molecular Biosciences, Washington State University, Pullman, WA, 991647520, USA.

[†]These authors contribute equally to this study.

[*]Correspondence: liuhuaiwei@sdu.edu.cn.

ABSTRACT

The long process of the assimilatory sulfate-reduction consists of sulfate reduction to H_2S and then H_2S assimilation for cysteine synthesis. The concept has not been challenged for a long time until now. Herein, phylogenetic analysis grouped assimilatory sulfite reductases into five clusters and we re-examined four representatives from two major clusters. These enzymes produced both zero valent sulfur (S^0) and H_2S from sulfite. However, S^0 was more like a direct product, while H_2S was just a derivative of S^0 via chemical reduction. Phylogenetic analysis of cysteine synthases grouped them into six clusters, and we re-examined six representatives from two major clusters. These enzymes used both glutathione persulfide (GSSH, a common intracellular compounds containing a S^0 atom) and H_2S as substrates to synthesize cysteine, but preferred to use GSSH. These findings challenged the long standing concept and supported that S^0, other than H_2S, is the key intermediate during the process of inorganic sulfur converting to organic sulfur.

IMPORTANCE

First, this study provides new insights into the sulfate reduction process. Representative sulfite reductases were investigated and both *in vitro* & *in vivo* tests proved they produce more zero valent sulfur (S^0) than H_2S from sulfite. S^0 is the direct product while H_2S is derivative of S^0. Second, this study provides new insights into cysteine synthesis pathway. Screening and analyses revealed that most cysteine synthases prefer S^0-containing compounds (e.g., GSSH) as substrate for cysteine synthesis. Together, the two findings indicate that S^0 is the key knot connecting sulfate reduction and cysteine synthesis, not the long believed H_2S.

KEYWORDS

Assimilatory sulfate-reduction, hydrogen sulfide, zero valent sulfur, sulfite reductase, cysteine synthase

INTRODUCTION

Sulfate reduction is a critical step of the sulfur biogeochemical cycle in which microorganisms play important roles. Depending on the fate of reduced sulfur atom, sulfate reduction process can be categorized into two types, dissimilatory sulfate reduction (DSR) and assimilatory sulfate reduction (ASR) (1, 2). DSR mainly happens in anaerobic environments where sulfate-reducing microorganisms (SOM) use sulfate as a terminal electron acceptor in the process of organic matter degradation, which results in the production of hydrogen sulfide (H_2S), in which the sulfur has a valence of -2. H_2S is released from SOM cells and is reoxidized in aerobic environments (1). Different from DSR, ASR is active in various environments where microorganisms use sulfate as a sulfur donor to synthesize organic compounds including cysteine, methionine, and glutathione. For ASR pathway, sulfate is first activated with ATP to form adenosine 5′-phosphosulfate (APS) and then to 3′-phosphoadenosine-5′-phosphosulfate (PAPS), which is reduced to sulfite. It is commonly believed that sulfite is finally reduced to H_2S, which then reacts with O-acetyl-serine (OAS) to produce cysteine (3-5). Hence, H_2S has been regarded as the key knot connecting sulfate-reduction and cysteine synthesis for over 60 years (6).

However, this opinion is facing an emerging challenge nowadays. Most of early studies that focus on sulfite reduction ignored the presence and involvement of zero valent sulfur (S^0), mainly due to lack of related knowledge of S^0 and its detection methods (7-11). Recent studies indicated that S^0 is widely present in all types of cells. It is not stable and can easily react with H_2S, small cellular thiols, such as glutathione

(GSH), and sulfite to form hydrogen polysulfides (HS_nH, n≥2), glutathione polysulfides (GS_nH, n≥2), and thiosulfate ($S_2SO_3^{2-}$) (12-14). These various forms are referred as sulfane sulfur (15, 16). In H_2S oxidation pathway, H_2S is firstly oxidized to S^0, and then to sulfite (17, 18). It is reasonable to assume that S^0 also exist in the ARS pathway. However, no such investigation has been reported.

It is well accepted that H_2S is the main substrate of cysteine synthases (19). Several studies indicate that some microbial cysteine synthases also can use thiosulfate ($S_2O_3^{2-}$), a relatively stable S^0 containing compound, as an alternative but less efficient substrate to produce cysteine (20, 21). In our previous study, we discovered that the *Schizosaccharomyces pombe* cysteine synthase Cys11 uses glutathione persulfide (GSSH) as a substrate to produce cysteine (22). Moreover, for Cys11, the K_m value of GSSH is ~400 μM, 2-fold lower than that of H_2S (~800 μM). Knocking out the sulfide:quinone oxidoreductase (Sqr), which converts H_2S to S^0 in mitochondria, leads to cysteine-deficient phenotypes. Therefore, we proposed that S^0 might be the *de facto* substrate of Cys11 inside of *S. pombe* cells. Whether Cys11 is an exception or it represents a common characteristic of microbial cysteine synthases needs further investigation.

In this study, we performed phylogenetic analysis of sulfite reductases and cysteine synthases. Representative enzymes were purified and their activities were examined. We found that all examined assimilatory sulfite reductases (aSiRs) produced more S^0 than H_2S from sulfite. H_2S was a derivative product of S^0. Microorganisms overexpressing aSiRs accumulated more S^0 than H_2S from sulfite reduction. All

representative cysteine synthases can use GSSH as a substrate to synthesize cysteine and most of them preferred GSSH to H_2S. These findings suggest that as in the H_2S oxidation pathway, S^0 also is the intermediate in the ASR pathway. S^0 is more like the key knot connecting sulfate reduction and cysteine synthesis other than H_2S.

Results

Methylene blue method cannot distinguish between hydrogen sulfide and hydrogen persulfide

Methylene blue method was commonly used in early studies of sulfite reductases. The mechanism is that two molecules of *N*,*N*-dimethyl-p-phenylenediamine (DMPD) and one H_2S molecule are oxidized by ferric ion (Fe^{3+}) to form a methylene blue dye, which has a maximal absorbance at around 670 nm (A_{670}) (Fig. 1). The A_{670} value is linearly correlated with amount of H_2S in the presence of excessive Fe^{3+}/DMDP (23, 24). We found that Fe^{3+}/DMPD not only reacted with H_2S, but also with hydrogen persulfide (HSSH). Furthermore, the latter generated higher A_{670} values than the former at the same doses (Fig. 1A). LC-ESI-MS analysis indicated that when H_2S reacted with Fe^{3+}/DMDP, not only methylene blue compound (**a**) was produced, another compound whose structure is similar as **a** but contains an extra sulfur atom (**b**) was also produced (Fig. S1). We proposed that **a** and **b** were generated from reactions 2 and 3, respectively (Fig. 1B). When HSSH reacted with Fe^{3+}/DMDP, **a** and **b** also were produced. The detailed mechanism was not investigated, but could be because HSSH is inherently unstable and easily breaks into H_2S and S^0 in aqueous solution, or

HSSH could react with Fe^{3+}/DMDP directly (reactions 4 and 5).

Elemental sulfur (S_8) did not generate any methylene blue dye, suggesting that only nucleophilic polysulfide (polysulfide with terminal hydrogen atoms) can react with Fe^{3+}/DMDP to produce S-containing heterocyclic dyes (Fig. 1B).

Representative aSiRs produced more S^0 than H_2S from sulfite *in vitro*

A total of 457,826 protein sequences are denoted as sulfite reductase in GenBank (update to August 29, 2024). These sequences were downloaded and subjected to redundancy analysis. After removing redundant sequences, 4,378 sulfite reductases were left. Their characteristic sequences were identified (PF01077 and PF03460) and using whether containing the identified characteristic sequences as a screening criterion, 289 sulfite reductases were finally extracted out. Origins of these enzymes encompass bacteria, archaea, fungi, and plants. Phylogenetic analysis of these enzymes indicated that 289 enzymes were categorized into five major clusters with clusters 3 and 4 were two largest ones (Fig. 2 and Table S1).

We chose four aSiRs as representatives for further examination: *E. coli* CysIJ (AAC75805.1), *S. cerevisiae* MET5&MET10 (NP_116579.1), and *S. pombe* Sir1 (CAB11176.1). They all belong to cluster 3; *Ruegeria pomeroyi* DSS-3 SPO2634 (AAV95879.1) belongs to cluster 4. Among them, CysIJ contains two subunits (Cys I and Cys J) and has been intensively studied as a model aSiR in 1960s. Others are from widely used model microorganisms. *S. cerevisiae* MET5&MET10 also contains two subunits, while *S. pombe* Sir1 and *R. pomeroyi* DSS-3 SPO2634 are single

subunit enzymes. These subunits/enzymes were fused with an N-terminal His-Tag, expressed in *E. coli* BL21(DE3), and purified using a nickel column (Fig. S2). During cell disruption and protein purification processes, no dithiothreitol (DTT) or other reductants was added. Freshly purified enzymes were immediately subjected to activity analysis.

We mixed purified CysI and CysJ to obtain the CysIJ complex. Likewise, the MET5&MET10 complex also was obtained. CysIJ, MET5&MET10, and Sir1 were NADPH dependent enzymes, we mixed them with NADPH and sulfite. SPO2634 was a ferredoxin dependent enzyme, we mixed it with ferredoxin (Fd), ferredoxin-NADP+ oxidoreductase (FNR), NADPH, and sulfite. The reactions were conducted at 25°C for 10 min. To analyze the produced sulfur compound, we used a LC-MS dependent method instead of the methylene blue method. The enzymatic products were derivatized with mBBr and analyzed using LC-ESI-MS. For the reaction catalyzed by CysIJ, H_2S derivatives mB-SH and mB-S-mB were detected. Signal intensity of the former was 1.9×10^6 and the latter was 4.6×10^5 (Fig. 3A, Fig. S3A and S3B). Surprisingly, derivative of HSSH (mB-SSH) also was detected and its signal intensity was 3.6×10^6 (Fig. 3A, Fig. S3C), higher than that of H_2S derivatives (mB-SH + mB-S-mB). Similarly, signal intensity of H_2S derivatives (mB-SH + mB-S-mB) from MET5&MET10 was 2.4×10^6; whereas signal intensity of HSSH derivative (mB-SSH) was 3.2×10^6 (Fig. 3B). Signal intensities of H_2S derivatives from SPO2634 and Sir1 also were lower than that of HSSH derivative (Fig. 3C and 3D).

To further confirm the S^0 products of these enzymes, we analyzed the products with another method. The reaction mixtures were reacted with methyl trifluoromethanesulfonate to convert hydrogen polysulfide (H_2S_n) to dimethylpolysulfide. Results showed that HSSH (H_2S_2) was the main product of these enzymes while HSSSSH (H_2S_4) was the minor one (Fig. 3E). We then quantified the produced S^0 with a cyanide method and compared it to the produced H_2S. Results showed that the former was much higher than the latter in all reaction systems (Fig. 3F and 3G), indicating that all of the four aSiRs produced more S^0 than H_2S.

For the presence of HS_nH in the products, a possible explanation is that aSiRs firstly produce H_2S from sulfite, and HS_nH are generated from autonomous oxidation of H_2S (by dissolved oxygen). However, according to our experience, the process of H_2S autonomous oxidation is slow, which usually takes hours without the help of related enzymes or strong oxidants (such as Fe^{3+} and H_2O_2). For confirmation, we mixed H_2S with reaction buffer containing no aSiR. After 10 min incubation at 25°C, no HS_nH was produced, suggesting that HS_nH was not produced from autonomous oxidation of H_2S. We also mixed HSSH with reaction buffer containing no aSiR. After 10 min incubation at 25°C, H_2S production was detected, whose amount was about 1/10 of HSSH, confirming that HSSH is inherently unstable in aqueous solution. After adding NADPH into the mixture, H_2S amount increased to about 1/2 of HSSH.

Together, the above results suggested that under the tested conditions *in vitro*, all of the four aSiRs catalyzed sulfite reduction to produce S^0. S^0 was more like the direct product of aSiRs, while H_2S was a derivative of S^0.

Representative aSiRs produced more S^0 than H_2S *in vivo*.

E. coli MG1655 contains no H_2S oxidation enzyme, which provides a clean background for testing the products of aSiRs. We expressed the four aSiRs (using the pBBR1MCS5 plasmid as a vector) in *E. coli* MG1655. *E. coli* MG1655 with the pBBR1MCS5 empty plasmid was used as a control. The cell suspension (10 ml, OD_{600}=3) was mixed with 0.5 mM sulfite in PBS buffer (pH 7.4, 50 mM) and the mixture was incubated at 37℃ with shaking. After 1 h incubation, consumed sulfite and generated products were quantified. We observed that compared with the control, all aSiR expression strains consumed more sulfite. More importantly, they all produced more total S^0 than H_2S from the consumed sulfite (Fig. 3H).

We also constructed a *S. cerevisiae* S288C strain (that contains no *sqr*) with MET5&MET10 overexpression and a *R. pomeroyi* DSS-3 Δ*sqr*Δ*fccAB* strain with SPO2634 overexpression (*sqr* and *fccAB* encode H_2S oxidation enzymes, their deletion makes H_2S cannot be oxidized to S^0 inside cells). Cell suspensions of these strains were mixed with sulfite, and the products were analyzed. Similarly, they also produced more S^0 than H_2S (Fig. 3I and 3J). These results demonstrated that the tested aSiRs tended to produce S^0 other than H_2S *in vivo*.

Representative cysteine synthases utilized S^0 to produce cysteine

A total of 499,263 protein sequences are denoted as cysteine synthase in GenBank (update to August 29, 2024). After removing redundant sequences, 1,159 cysteine

synthases were left. We identified the characteristic sequence (PF00291) from them. Using whether containing the identified characteristic sequence as a screening criterion, 735 cysteine synthases were finally extracted out. Origins of these enzymes encompass bacteria, archaea, fungi, and plants. Phylogenetic analysis of these enzymes indicated that they were categorized into six major clusters with clusters 4 and 5 were two largest ones (Fig. 4, Table S2).

We selected 5 microbial cysteine synthases for further study: CysK and CysM from *E. coli* MG1655 (EcCysK and EcCysM), CysK from *R. pomeroyi* DSS-3 (RpCysK), SiRe_1641 from *Sulfolobus islandicus* REY15A, a model archaeon that belongs to Crenarchaeota. They all belong to cluster 4. CysM from *R. pomeroyi* DSS-3 (RpCysM) belongs to cluster 5. We expressed their encoding genes in *E. coli* BL21(DE3). These enzymes (fused with a His-tag at N-terminus) were purified using a nickel column (Fig. S4). Freshly purified enzymes were subjected to activity analysis immediately.

A catalyzing mechanism of cysteine synthase has been reported. OAS first reacted with PLP to form the α-aminoacrylate intermediate containing a C=C bond, which was electrophilic. Subsequently, nucleophilic H_2S attacked the C=C bond of α-aminoacrylate to generate cysteine (Fig. 5) (25). We mixed purified cysteine synthases with H_2S/GSSH/$Na_2S_2O_3$, OAS, and pyridoxal 5-phosphate (PLP) in PBS buffer (50 mM, pH 7.4) and incubated the mixture at 30°C for 5 min. LC-ESI-MS method was used to analyze the products.

From the catalyzing mechanism perspective, GSSH and $Na_2S_2O_3$ react with OAS

will generate GS-cysteine and sulfo-cysteine intermediates, respectively. We detected these two intermediates from reactions catalyzed by all five enzymes (Fig. S5-S10). L-cysteine (derivatized by bimane) also was detected from H_2S participating reaction catalyzed by these enzymes (Fig. S5-S10).

We then assayed the kinetics of all five cysteine synthases (Fig. 6, Fig. S11-S13). The obtained data were compared with the reported data of *S. pombe* cysteine synthase Cys11 (22). For all 6 enzymes, the K_m values for GSSH were between 202~426 μM, K_m values for H_2S were between 157~3192 μM, and K_m values for $Na_2S_2O_3$ were between 408~3774 μM. The V_{max} values for GSSH were between 0.125~0.280 mM·min^{-1}, V_{max} values for H_2S were between 0.139~0.581 mM·min^{-1}, and V_{max} values for $Na_2S_2O_3$ were between 0.021~0.173 mM·min^{-1}. The K_{cat} values for GSSH were between 2.083~9.778 s^{-1}, K_{cat} values for H_2S were between 3.127~13.833 s^{-1}, and K_{cat} values for $Na_2S_2O_3$ were between 0.495~2.454 s^{-1}. These results indicated that among GSSH, H_2S, and $Na_2S_2O_3$, $Na_2S_2O_3$ was the most unpreferred substrate. Most cysteine synthases showed higher affinity to GSSH than to H_2S.

DISCUSSION

Inorganic sulfur (sulfate) becomes organic sulfur (cysteine) via the assimilatory sulfate reduction and cysteine synthesis pathways. The concept that H_2S is a key intermediate of this process is founded in 1960s when S^0 analysis methods were short and knowledge of biological S^0 were scarce (6). In this study, we re-examined the

product of aSiRs with modern methods that can distinguish S^0 containing compounds from H_2S. We found that all tested aSiRs produced both S^0 and H_2S from sulfite. S^0 was more like the direct product of aSiRs while H_2S was its derivative. We also re-examined model cysteine synthases and discovered that all tested cysteine synthases can use S^0 ($S_2O_3^{2-}$ and GSSH) as alternative substrates to produce cysteine.

In recent years, a number of H_2S producing enzymes have been redefined as S^0 producing enzymes thanks to the development of S^0 analysis methods. For instance, 3-mercaptopyruvate sulfurtransferase (3-MST), which was reported to cleave the C–S bond of 3-mercaptopyruvate to produce H_2S. In 2015, Kimura *et al*., discovered that the released sulfur atom actually existed as HS_nH (26). Cystathionine β-synthetase (CBS) and cystathionine γ-lyase (CSE) both produced S^0 from cystine (27, 28). Methanethiol oxidase (MTO) catalyzed methanethiol degradation to produce S^0 other than previously reported H_2S (29). From sulfur cycle viewpoint, these findings indicate that when organic sulfur is converted to inorganic sulfur by biological systems, S^0 is the direct product. Therefore, it is somehow strange that S^0 is skipped when inorganic sulfur is converted to organic sulfur by the same biological systems. In addition, since S^0 has been recognized as the key intermediate of H_2S oxidation pathway, it is confusing why S^0 is not present in the sulfur reduction pathway. The findings that S^0 is the direct product of aSiRs can well explain these confusions.

From chemistry viewpoint, biological S^0 compounds are better intermediates than H_2S. First, the pK_a1 of H_2S is 6.8 and gasification temperature is 34.3°C, so it easily releases out of cells under normal physiological condition. In comparison, the pK_a of

GSSH is 5~6, it mainly exist in deprotonated form inside cells (30). Thiosulfate is even more stable than GSSH. Second, H_2S is toxic to the respiration system, its intracellular concentration is limited to 10~30 nM level (31), which was far below the K_m value of cysteine synthases. In contrast, intracellular S^0 chemicals are high to 100~400 μM (31, 32), which was near the K_m values of cysteine synthases. Third, biological S^0 compounds have distinctive activities. For instance, GSSH is more nucleophilic than GSH because of the α-effect and hence displays high reactivity toward electrophiles such as reactive oxygen species (ROS) and toxic metal cations (33). In consistent, we found that cysteine synthases preferred GSSH the most. We also found that microorganisms accumulated high concentration of intracellular S^0 during the fast growth phase (cysteine synthesis process is active in fast growth phase), but reduced its level quickly after that (32). Combining the above evidence, we proposed that S^0 is the *de facto* substrate of cysteine synthases *in vivo*. Thus, S^0 probably is a key knot connecting sulfate reduction and cysteine synthesis in microorganisms. H_2S is more like an efflux of intracellular S^0 (Fig. 7).

MATERIALS AND METHODS

Strains and cultivation conditions.

R. pomeroyi DSS-3 is a gift from Prof. Yuzhong Zhang of Ocean University of China. *R. pomeroyi* DSS-3 derivative Δ*sqr*Δ*fccAB* were constructed in a previous work(29). *S. islandicus* REY15A is a gift from Prof. Yulong Shen of Shandong University. *S. pombe* YHL6381 is a gift from Prof. Huang Ying. *E. coli* strains used for plasmid

construction and protein expression, and plasmids constructed in this study are all listed in Table S4. *E. coli* strains were cultured in LB medium. *R. pomeroyi* DSS-3 strains were cultured in 1/2 YTSS medium. *S. cerevisiae* S288C strains were cultured in YPD or SD medium. *S. pombe* YHL6381 strains were cultured in YES or SD medium. *S. islandicus* REY15A were grown in MTSV medium [mineral salt supplemented with 0.2% w/v (weight/volume) tryptone (T), 0.2% (w/v) sucrose (S), mixed solution of vitamins (V)] or MTSVU medium [MTSV supplemented with 0.001% (w/v) uracil (U)]. For cultivation, *E. coli* strains were cultured at 37℃ with shaking (220 rpm). *R. pomeroyi* DSS-3, *S. cerevisiae* S288C and *S. pombe* YHL6381 strains were cultivated at 30℃ with shaking (220 rpm). *S. islandicus* REY15A strains were cultivated at 75℃ with shaking (220 rpm).

Reagents

Sodium hydrosulfide (NaHS), cysteine, reduced glutathione (GSH), sulfite and thiosulfate were purchased from Sigma-Aldrich (Saint Louis, MO). S_8 were purchased from TCI Company (Shanghai, China). HS_nH was prepared following the protocol of Luebke *et al* (34). GSSH was prepared following the protocol of Visser *et al* (35). Briefly, the elemental sulfur (S_8) was dissolved in acetone to make a saturated sulfur solution (~17 mM). GSH was dissolved in distilled water (17 mM). The two solutions were mixed at 1:1 ratio (volume) in 100 mM Kpi buffer (pH 7.4) to make GSSH (~4 mM). Other chemicals were purchased from local companies if not specifically mentioned.

Methylene blue method

The methylene blue method was performed as reported previously (23). Two reagents were required, 0.02 M *N*,*N*-dimethyl-p-phenylenediamine sulfate in 7.2 N hydrochloric acid (DPD reagent), and 0.03 M ferric chloride in 1.2 N hydrochloric acid (ferric chloride agent). Assays are performed in 1.5-mL microfuge tubes. First, 250 μl deionized water was added into a 1.5-ml tube, followed by the addition of 250 μl NaHS, HSSH, or S_8 solution (in 50 μM, 100 μM, 200 μM, or 500 μM concentration). Second, 20 μl DPD reagent was added, rapidly followed by addition of 20 μl of ferric chloride reagent. The mixture was shaken vigorously and placed in the dark for 30 minutes. After being centrifuged at 17,000 × *g* for 2 minutes. Supernatant (200 μl) was pipetted out and the absorbance at 670 nm was measured. The compounds in supernatant were analyzed using LC-ESI-MS.

LC-ESI-MS Analysis

The quadrupole time-of-flight, high-resolution mass spectrometer (Ultimate 3000, Burker impact HD, Thermo Fisher, Waltham, MA, USA) was used. The column was InertSustain C18 5 μm (4.6 mm × 250 mm, GL Sciences, Shanghai, China). Injection volume of sample was 10 μl. The source temperature was set at 200°C and the ion spray voltage was at 4.5 kv. Nitrogen was used as the nebulizer and drying gas. The mobile phase was a mixture of pure water and methanol. A linear gradient of solvent A (0.25% acetic acid in ddH2O) and solvent B (100% methanol) from 7.5% to 100%

to 7.5% (solvent B) in 31 min was used for elution, the column temperature was maintained at 38°C. Data were acquired in full MS (100−1500 m/z) mode. Full mass resolution (40000@ m/z 1222) at full sensitivity.

Phylogenetic analysis

The protein sequences of sulfite reductase and cysteine synthase were downloaded from NCBI database (update to 29 August 2024). Redundant sequences were removed using the CD-hit tool with conventional criteria (sequence identity threshold ≥45%, word length =2). The characteristic sequences of the conserved regions were analyzed in the InterPro database. The characteristic sequences of sulfite reductases were PF01077 and PF03460, and the characteristic sequences of cysteine synthases was PF00291. The hmmsearch command in Hmmer tool was used to identify all the featured sequences. Phylogenetic trees were constructed by a neighbor-joining method using ETE3 with a partial deletion, p-distance distribution, and bootstrap at 1,000 repeats. Multiple sequence alignment was performed using MUSCLE.

Protein expression and purification

Cysteine synthases and sulfite reductases encoding genes were amplified from genomic DNA of *E. coli*, *R. pomeroyi* DSS-3, *S. cerevisiae* S288C, *S. pombe* YHL6381 and *S. islandicus* REY15A genomic DNA. The expression plasmids (see Table S4) were constructed using primers listed in Table S5. These plasmids were introduced into *E. coli* BL21(DE3) and the strains were incubated in LB medium

containing kanamycin (50 μg/ml). When OD_{600} reached 0.6, 0.4 mM isopropyl β-D-1-thiogalactopyranoside (IPTG) was added and the temperature was decreased to 25°C. The cultivation was further continued overnight. Cells were harvested by centrifugation and then re-suspended in binding buffer (200 mM NaCl, 50 mM NaH_2PO_4, 20 mM Imidazol, pH 8.0). For protein purification, cell disruption was performed using a Pressure Cell Homogeniser (SPCH-18) at 4°C. Cell lysate was centrifuged to remove the debris and cysteine synthetase/sulfite reductase was purified using the nickel-nitrilotriacetic acid (Ni-NTA) agarose resin (Invitrogen, Waltham, MA, USA). Purification was conducted by following the manufacturer's instructions. The eluted protein was loaded onto the PD-10 desalting column (GE) for buffer exchange to sodium phosphate buffer (20 mM, pH 7.6). Purity of the proteins was examined via SDS-PAGE.

Sulfite reductase activity assay *in vitro*

The assays were performed as previously reported (8). Briefly, for CysIJ, Met5&Met10, and Sir1 activity assays, 0.3 ml reaction buffer (50 mM K_3PO_4, pH 7.7, containing 0.1 mM Na_2EDTA) contained 2 mg/ml purified sulfite reductase, 100 μM sulfite, 100 μM hemin and 2 mM NADPH. The reaction was conducted at 25°C for 10 min. For SPO2634 activity assay, 0.3 ml Tris-HCl buffer (pH 7.5, containing 0.1 M NaCl) contained 2 mg/ml SPO2634 crude enzyme or 0.2 mg/ml purified SPO2634, 0.5 mg/ml purified ferredoxin (Fd, SPO2377), 0.1 mg/ml purified ferredoxin-NADP reductase (FNR, SPO2637), 200 μM sulfite and 2 mM NADPH. The reaction was conducted at 25°C for 10 min.

Produced S^0 in the reaction solution was analyzed by two methods. The cyanide method for quantification (36) and a HPLC based method for species determination (37). Produced H_2S and remaining sulfite in the reaction solution were labeled with monobromobimane (mBBr) following a previously reported protocol (18), and then were quantified by LC-ESI-MS as described above.

Sulfite reductase activity assay *in vivo*

E. coli MG1655-CysJI/Met5&Met10/Sir1 overexpression strains were constructed with pBBR1MCS5 plasmids (Table S4). The strains were cultured in LB medium at 37°C for overnight. The overnight culture (1 ml) was transferred into 100 ml fresh LB medium and cultured to OD_{600}=0.4, and then 0.4 mM IPTG was added and the cultivation continued at 37°C for 3.5 h. Cells were collected by centrifugation (4,500×*g*, 10 min) and re-suspended in PBS buffer (pH 7.4, 50 mM) to make a OD_{600}=3.0 cell suspension. Sulfite (0.5 mM) was added into 10 ml cell suspension in a 50-ml scale tube. The tube was then incubated at 37℃ for 1 h with shaking (200 rpm).

R. pomeroyi-SPO2634 overexpression strains were constructed with *R. pomeroyi* DSS-3 Δ*sqr*Δ*fccAB* strain and pBBR1-SPO2634 plasmid (Table S4). Strains were cultured in 1/2 YTSS medium at 30℃ for overnight. The overnight culture (1 ml) was transferred into 100 ml of fresh medium and cultured to OD_{600}= 0.7, and then 0.1 mM sulfite was added and the cultivation continued until OD_{600} reached 2.0. Cells were collected by centrifugation (4,500×*g*, 10 min) and re-suspended in Tris-HCl buffer (pH 8.4, 50 mM, 20 mM $MgCl_2$, 20g/L NaCl) to make a OD_{600}=5.0 cell suspension. Sulfite (0.5 mM) was added into 10 ml cell suspension in a 50-ml scale tube. The tube was then incubated at 30℃ for 1 h with shaking (200 rpm).

S. cerevisiae S288C-MET5&MET10 overexpression strain was constructed with pJFE3 vector (Table S1). The strain was cultured in SD-URA medium at 30℃ for overnight. The overnight culture (1 ml) was transferred into 100 ml of fresh medium and cultured to OD_{600}= 0.6, and then 0.1 mM sulfite was added and the cultivation continued until OD_{600} reached 1.0. Cells were collected by centrifugation (4,500×*g*, 10 min) and re-suspended in PBS buffer (pH 7.4, 50 mM) to make a OD_{600}=10.0 cell suspension. Sulfite (0.5 mM) was added into 10 ml cell suspension in a 50-ml scale tube. The tube was then incubated at 30℃ for 1 h with shaking (200 rpm).

To quantify the consumed sulfite and produced H_2S in cell suspensions, the cell suspensions were centrifuged (4,500×*g*, 10 min) and 50 μl supernatant was taken after centrifugation. The supernatant was derivatized with mBBr and then quantified by HPLC following a reported protocol (18). The produced S^0 was quantified with the cyanide method.

Cysteine synthase activity assay

Cysteine synthases were expressed in *E. coli* BL21(DE3) (Table S4) and purified with Ni-NTA agarose resin. Activity assay was carried out as described previously. Briefly, 0.3 ml reaction buffer (50 mM PBS buffer, pH 7.4) contained 1 mg/ml purified enzyme, 100 μM pyridoxal phosphate, 1.0 mM–2.0 mM O-acetyl-L-serine (OAS), 1.0–5.0 mM NaSH, GSSH, or $Na_2S_2O_3$. The reaction was conducted at 30°C for 5 min and the products were derivatized with mBBr and analyzed with LC-ESI-MS. For kinetics assay, the same reaction system contained varied concentrations of NaSH, GSSH or $Na_2S_2O_3$ (see maintain text). The reaction was conducted at 30°C for 5 min. For the reaction using NaSH as a substrate, the produced cysteine was labeled with mBBr and quantified by HPLC. For the reaction using GSSH or thiosulfate as a

substrate, after 5 min reaction, the product was mixed with 0.5 mM tris-(2-carboxyethyl)-phosphine (TCEP), and the released cysteine was labeled with mBBr and quantified by HPLC. All kinetic parameters were determined using the Michaelis-Menten equation (non-linear regression) embedded in Graphpad prism software.

ACKNOWLEDGEMENTS

This work was supported by the National Key R&D Program of China (2022YFC3401301) and the National Natural Science Foundation of China (92351302).

DECLARATION OF COMPETING INTEREST

The authors declare no conflict of interest regarding the publication of this article.

REFERENCES

1. Jorgensen BB, Findlay AJ, Pellerin A. 2019. The biogeochemical sulfur cycle of marine sediments. Front Microbiol 10:849.
2. Wu B, Liu F, Fang W, Yang T, Chen GH, He Z, Wang S. 2021. Microbial sulfur metabolism and environmental implications. Sci Total Environ 778:146085.
3. Jespersen M, Wagner T. 2023. Assimilatory sulfate reduction in the marine methanogen *Methanothermococcus thermolithotrophicus*. Nat Microbiol 8:1227-1239.
4. Takahashi H, Kopriva S, Giordano M, Saito K, Hell R. 2011. Sulfur assimilation in photosynthetic organisms: molecular functions and regulations of transporters and assimilatory enzymes. Annu Rev Plant Biol 62:157-184.

5. Demin KA, Prazdnova EV, Minkina TM, Gorovtsov AV, Reguera G. 2024. Sulfate-reducing bacteria unearthed: ecological functions of the diverse prokaryotic group in terrestrial environments. Appl Environ Microbiol 90:e139023.
6. PASTERNAK CA, ELLIS RJ, JONES-MORTIMER MC, CRICHTON CE. 1965. The control of sulphate reduction in bacteria. Biochem J 1:270-275.
7. Kline BC, Schoenhard DE. 1970. Biochemical characterization of sulfur assimilation by *Salmonella pullorum*. J Bacteriol 1:142-150.
8. Ostrowski J, Barber MJ, Rueger DC, Miller BE, Siegel LM, Kredich NM. 1989. Characterization of the flavoprotein moieties of nadph-sulfite reductase from *Salmonella typhimurium* and *Escherichia coli*: Physico-chemical and catalytic properties, amino acid sequence deduced from dna sequence of *cysJ*, and comparison with nadph-cytochrome P-450 reductase. J Biol Chem 264:15796-15808.
9. Lewis MS, Patricia SD, Henry K. 1974. Reduced Nicotinamide Adenine Dinucleotide Phosphate-Sulfite Reductase of Enterobacteria: III. THE *ESCHERICHIA COLI* HEMOFLAVOPROTEIN: CATALYTIC PARAMETERS AND THE SEQUENCE OF ELECTRON FLOW. Journal of Biological Chemistry Volume 249:1572-1586.
10. Covès J, Nivière V, Eschenbrenner M, Fontecave M. 1993. NADPH-sulfite reductase from Escherichia coli. A flavin reductase participating in the generation of the free radical of ribonucleotide reductase. J Biol Chem 268:18604-18609.
11. Siegel LM, Leinweber FJ, Monty KJ. 1965. Characterization of the Sulfite and Hydroxylamine Reductases of *Neurospora crassa*. J Biol Chem 240:2705-2711.
12. Ogata S, Matsunaga T, Jung M, Barayeu U, Morita M, Akaike T. 2023. Persulfide

biosynthesis conserved evolutionarily in all organisms. Antioxid Redox Signal 39:983-999.

13. Lau N, Pluth MD. 2019. Reactive sulfur species (RSS): persulfides, polysulfides, potential, and problems. Curr Opin Chem Biol 49:1-8.
14. Filipovic MR, Zivanovic J, Alvarez B, Banerjee R. 2018. Chemical biology of H_2S signaling through persulfidation. Chem Rev 118:1253-1337.
15. Sawa T, Takata T, Matsunaga T, Ihara H, Motohashi H, Akaike T. 2021. Chemical biology of reactive sulfur species: hydrolysis-driven equilibrium of polysulfides as a determinant of physiological functions. Antioxid Redox Signal 36:327-336.
16. Olson KR. 2019. Hydrogen sulfide, reactive sulfur species and coping with reactive oxygen species. Free Radic Biol Med 140:74-83.
17. Giedroc DP. 2017. A new player in bacterial sulfide-inducible transcriptional regulation. Mol Microbiol 105:347-352.
18. Xin Y, Liu H, Cui F, Liu H, Xun L. 2016. Recombinant *Escherichia coli* with sulfide:quinone oxidoreductase and persulfide dioxygenase rapidly oxidises sulfide to sulfite and thiosulfate via a new pathway. Environ Microbiol 18:5123-5136.
19. Becker MA, Kredich NM, Tomkins GM. 1969. The purification and characterization of O-acetylserine sulfhydrylase-A from *Salmonella typhimurium*. J Biol Chem 244:2418-2427.
20. Nakamura T, Iwahashi H, Eguchi Y. 1984. Enzymatic proof for the identity of the S-sulfocysteine synthase and cysteine synthase B of *Salmonella typhimurium*. J Bacteriol 158:1122-1127.
21. Hensel G, Truper HG. 1983. O-Acetylserine sulfhydrylase and S-sulfocysteine

synthase activities of *Rhodospirillum tenue*. Arch Microbiol 134:227-232.

22. Zhang X, Xin Y, Chen Z, Xia Y, Xun L, Liu H. 2021. Sulfide-quinone oxidoreductase is required for cysteine synthesis and indispensable to mitochondrial health. Redox Biol 47:102169.
23. Siegel LM. 1965. A direct microdetermination for sulfide. Anal Biochem 11:126-132.
24. Kubán V, Dasgupta PK, Marx JN. 1992. Nitroprusside and methylene blue methods for silicone membrane differentiated flow injection determination of sulfide in water and wastewater. Analytical chemistry (Washington) 64:36-43.
25. Claus MT, Zocher GE, Maier TH, Schulz GE. 2005. Structure of the O-acetylserine sulfhydrylase isoenzyme CysM from *Escherichia coli*. Biochemistry 44:8620-8626.
26. Kimura Y, Toyofuku Y, Koike S, Shibuya N, Nagahara N, Lefer D, Ogasawara Y, Kimura H. 2015. Identification of H_2S_3 and H_2S produced by 3-mercaptopyruvate sulfurtransferase in the brain. Sci Rep 5:14774.
27. Mishanina TV, Libiad M, Banerjee R. 2015. Biogenesis of reactive sulfur species for signaling by hydrogen sulfide oxidation pathways. Nat Chem Biol 11:457-464.
28. Kimura H. 2021. Hydrogen Sulfide (H_2S) and Polysulfide (H_2S_n) Signaling: The First 25 Years. Biomolecules 11:896.
29. Cao Q, Liu X, Wang Q, Liu Z, Xia Y, Xun L, Liu H. 2024. Rhodobacteraceae methanethiol oxidases catalyze methanethiol degradation to produce sulfane sulfur other than hydrogen sulfide. mBio 15:e02907-23.
30. Benchoam D, Semelak JA, Cuevasanta E, Mastrogiovanni M, Grassano JS, Ferrer-Sueta G, Zeida A, Trujillo M, Möller MN, Estrin DA, Alvarez B. 2020. Acidity and nucleophilic reactivity of glutathione persulfide. Journal of Biological

Chemistry 295:15466-15481.

31. Kimura H. 2015. Signaling molecules: hydrogen sulfide and polysulfide. Antioxid Redox Signal 22:362-376.

32. Ran M, Wang T, Shao M, Chen Z, Liu H, Xia Y, Xun L. 2019. Sensitive method for reliable quantification of sulfane sulfur in biological samples. Anal Chem 91:11981-11986.

33. Bianco CL, Chavez TA, Sosa V, Saund SS, Nguyen QNN, Tantillo DJ, Ichimura AS, Toscano JP, Fukuto JM. 2016. The chemical biology of the persulfide (RSSH)/perthiyl (RSS·) redox couple and possible role in biological redox signaling. Free Radic Biol Med 101:20-31.

34. Luebke JL, Shen J, Bruce KE, Kehl-Fie TE, Peng H, Skaar EP, Giedroc DP. 2014. The CsoR-like sulfurtransferase repressor (CstR) is a persulfide sensor in *Staphylococcus aureus*. Mol Microbiol 94:1343-1360.

35. Visser JM, Robertson LA, Van Verseveld HW, Kuenen JG. 1997. Sulfur Production by Obligately Chemolithoautotrophic *Thiobacillus* Species. Appl Environ Microbiol 63:2300-2305.

36. Bartlett JK, Skoog DA. 1954. Colorimetric determination of elemental sulfur in hydrocarbons. Anal Chem 26:1008-1011.

37. Kamyshny AJ, Goifman A, Gun J, Rizkov D, Lev O. 2004. Equilibrium Distribution of Polysulfide Ions in Aqueous Solutions at 25 °C: A New Approach for the Study of Polysulfides' Equilibria. Environ Sci Technol 38:6633-6644.

FIGURE LEGENDS

FIG 1. Application of methylene blue method in H2S and S0 quantification; (A) HSSH and H_2S can react with methylene blue reagents to generate thiaazaheterocyclic dyes but S_8 cannot. Data are from three replicated experiments (n=3) and presented as average ± s.d; (B) Mechanisms of how HSSH and H_2S react with methylene blue reagents. Reactions 1 and 2 are from reference (24). Other reactions are proposed by authors.

FIG 2. Phylogenetic analysis of 289 sulfite reductases. Only part origins of the enzymes were shown. Details of these enzymes and their origins are shown in Table S1.

FIG 3. Analysis of the products generated from sulfite reductase-catalyzed reactions; Purified CysIJ (A), MET5&10 (B), and SPO2634 (C) were mixed with NADPH and

sulfite; purified Sir1 (D) was mixed with ferredoxin, ferredoxin-NADP+ oxidoreductase, NADPH, and sulfite. The reactions were conducted at 25°C for 10 min. Products were derivatized by mBBr. After mBBr derivatization, H_2S became mB-SH and mB-S-mB, and HSSH became mB-SSH. The derivatives were detected by LC-ESI-MS. MS signal intensities of H_2S (mB-SH + mB-S-mB) and HSSH (mB-SSH) were shown. MS spectra of these chemicals were shown in Fig. S3; (E) The enzyme-produced H_2S_n was derivatized by methyl trifluoromethanesulfonate and analyzed using HPLC with UV detection. H_2S_n mixture was used as the standard; (F) The enzyme-produced H_2S_n was quantified using cyanide method and shown as total S^0; (G) The enzyme-produced H_2S was quantified by HPLC; (H) Sulfite consumption, S^0 production, and H_2S production from *E. coli* MG1655 strains overexpressing sulfite reductases; (I) Sulfite consumption, S^0 production, and H_2S production from *S. cerevisiae* S288C overexpressing MET5&10; (J) Sulfite consumption, S^0 production, and H_2S production from *R. pomeroyi* DSS-3Δ*sqr*Δ*fccAB* overexpressing SPO2634. Controls are strains without sulfite reductase overexpression. For F–J, data are from three replicated experiments (n=3) and presented as average ± s.d. T-tests were performed to calculate the p-values. Asterisks indicate statistically significant difference (* $p < 0.05$, ** $p < 0.01$, ***$p < 0.001$, ****$p < 0.0001$).

FIG 4. Phylogenetic analysis of 735 cysteine synthases. Only part origins of the enzymes were shown. Details of these enzymes and their origins are shown in Table S2.

FIG 5. Proposed mechanism of how cysteine synthase using different sulfur donors to produce cysteine and its intermediates.

FIG 6. Kinetic assays of cysteine synthases with different substrates. Details of the data are shown in Table S3 and Fig. S11–S13.

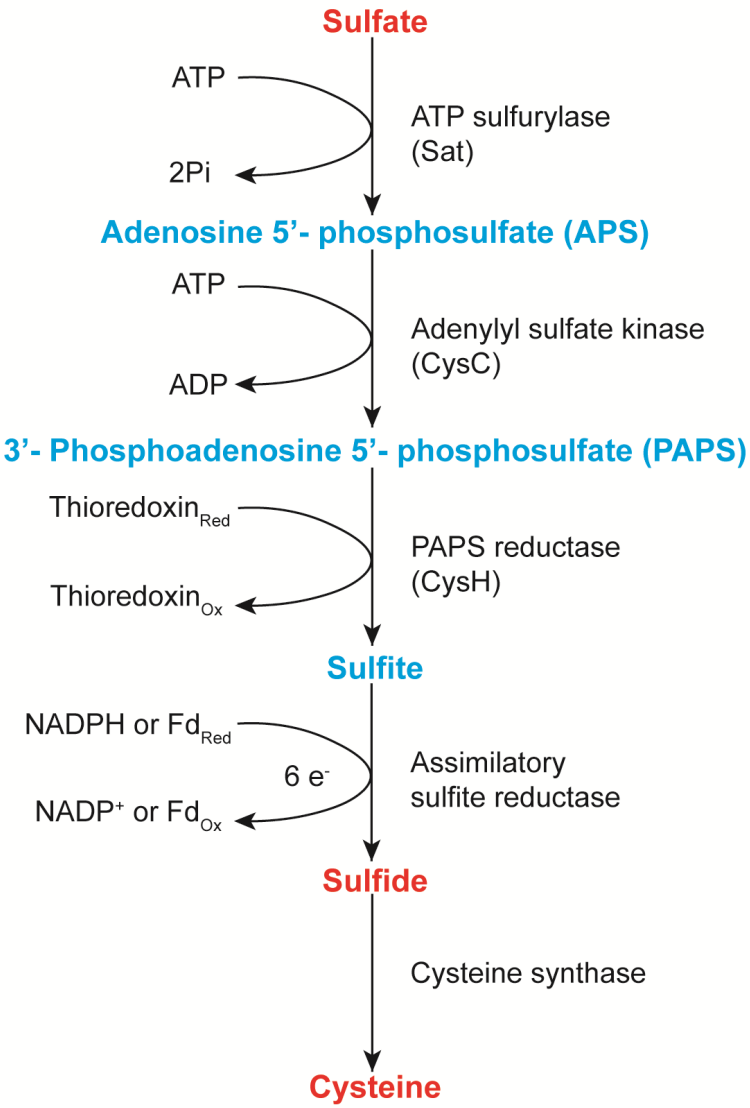
Sulfate
ATP
2Pi
ATP sulfurylase
(Sat)
Adenosine 5'- phosphosulfate (APS)
ATP
ADP
Adenylyl sulfate kinase
(CysC)
3'- Phosphoadenosine 5'- phosphosulfate (PAPS)
Thioredoxin$_{Red}$
Thioredoxin$_{Ox}$
PAPS reductase
(CysH)
Sulfite
NADPH or Fd$_{Red}$
6 e$^-$
NADP$^+$ or Fd$_{Ox}$
Assimilatory
sulfite reductase
Sulfide
Cysteine synthase
Cysteine

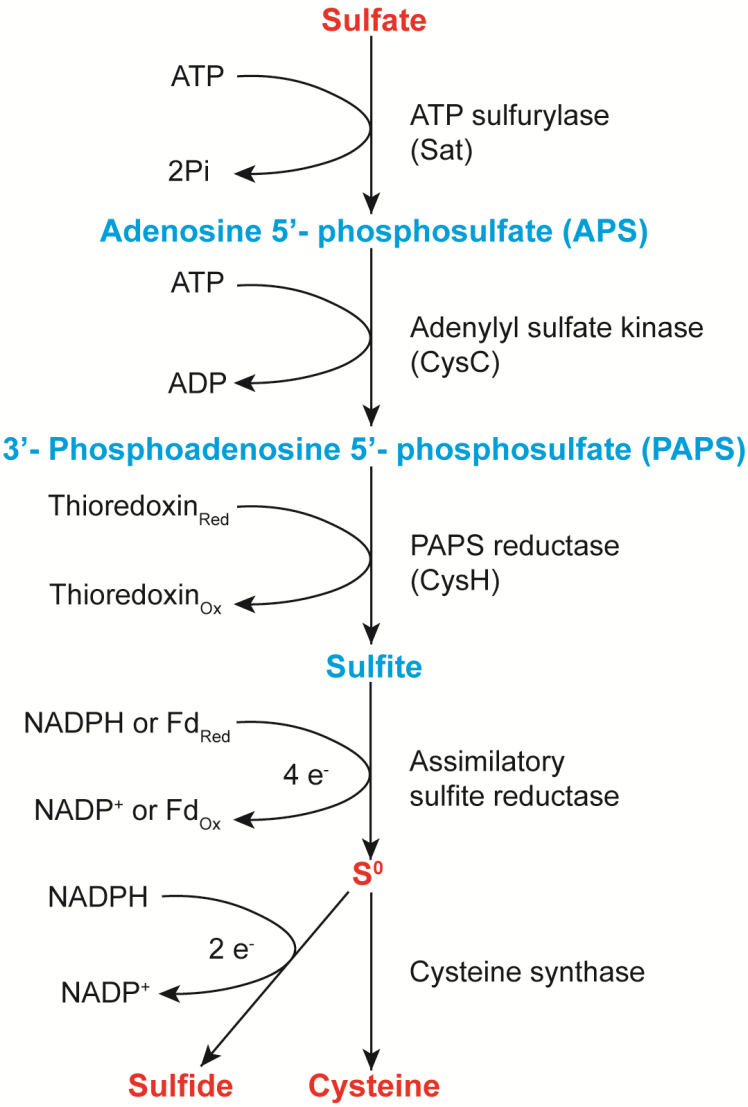
Sulfate
ATP
2Pi
ATP sulfurylase
(Sat)
Adenosine 5'- phosphosulfate (APS)
ATP
ADP
Adenylyl sulfate kinase
(CysC)
3'- Phosphoadenosine 5'- phosphosulfate (PAPS)
Thioredoxin$_{Red}$
Thioredoxin$_{Ox}$
PAPS reductase
(CysH)
Sulfite
NADPH or Fd$_{Red}$
4 e$^-$
NADP$^+$ or Fd$_{Ox}$
Assimilatory
sulfite reductase
S^0
NADPH
2 e$^-$
NADP$^+$
Cysteine synthase
Sulfide
Cysteine

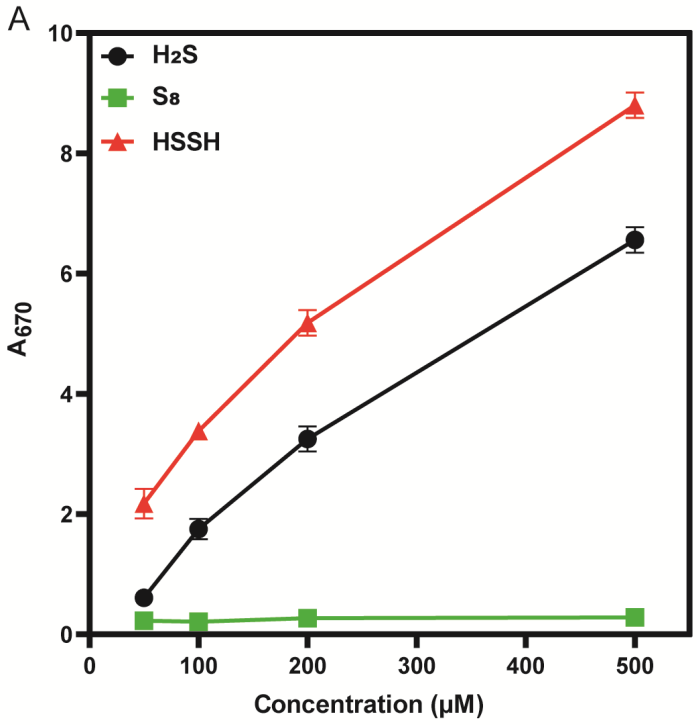
A
H2S
S8
HSSH
A670
Concentration (μM)
0
100
200
300
400
500
0
2
4
6
8
10

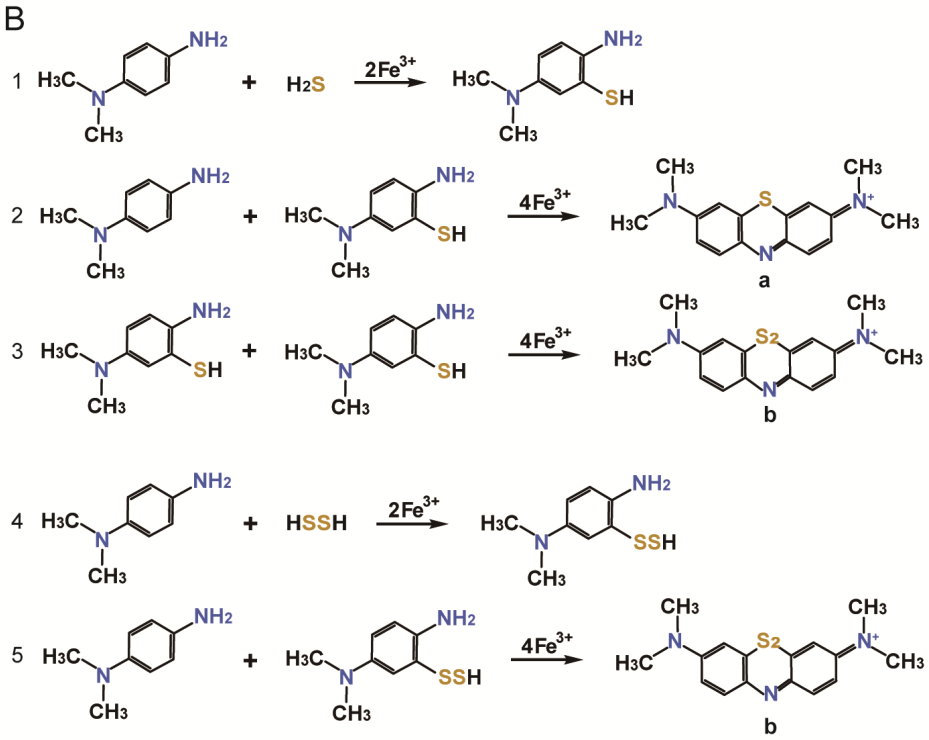
B
1
2
3
4
5
H2S
HSSH
2Fe3+
4Fe3+
NH2
SH
SSH
S2
a
b

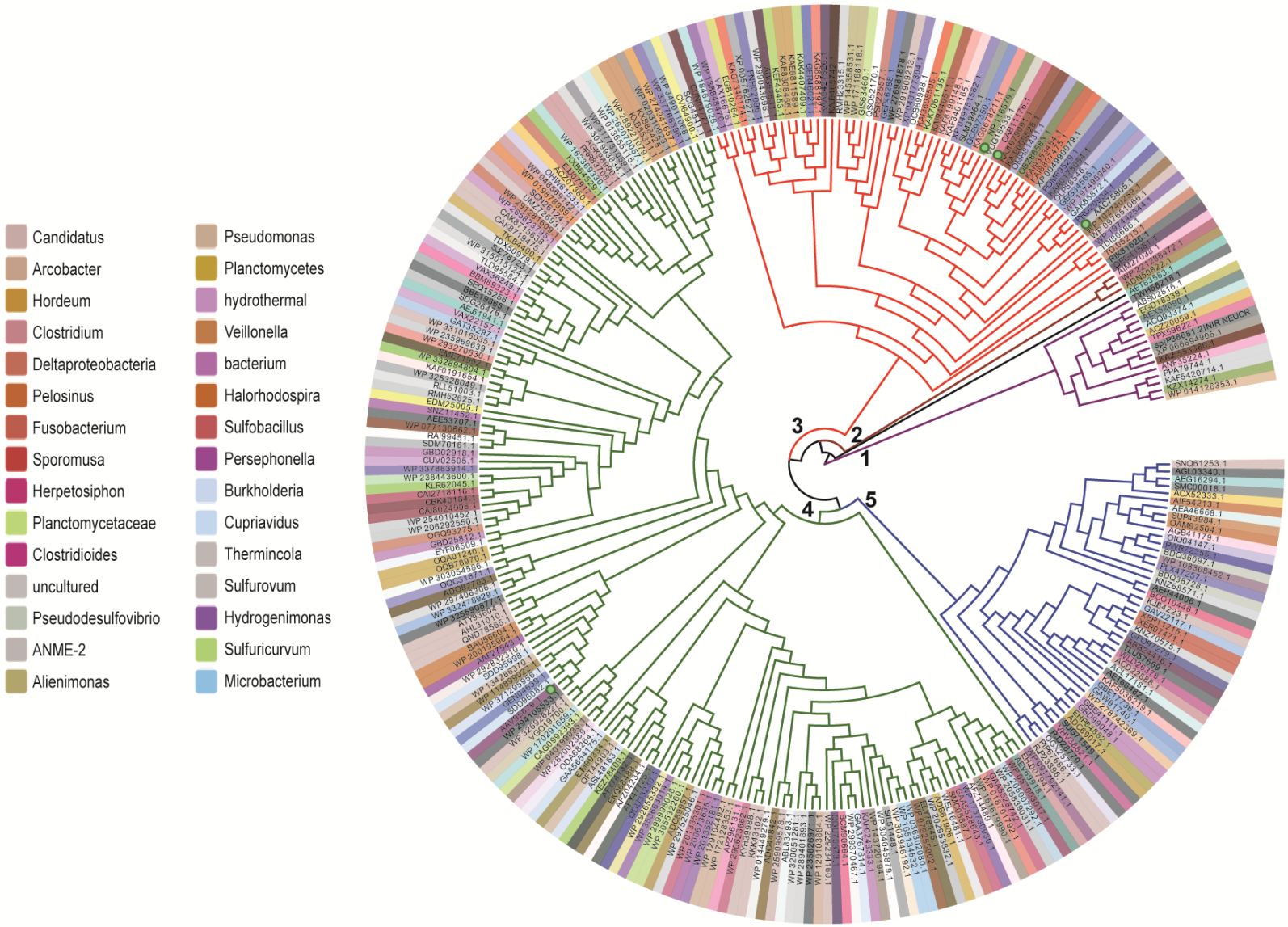
Candidatus
Arcobacter
Hordeum
Clostridium
Deltaproteobacteria
Pelosinus
Fusobacterium
Sporomusa
Herpetosiphon
Planctomycetaceae
Clostridioides
uncultured
Pseudodesulfovibrio
ANME-2
Alienimonas
Pseudomonas
Planctomycetes
hydrothermal
Veillonella
bacterium
Halorhodospira
Sulfobacillus
Persephonella
Burkholderia
Cupriavidus
Thermincola
Sulfurovum
Hydrogenimonas
Sulfuricurvum
Microbacterium
1
2
3
4
5

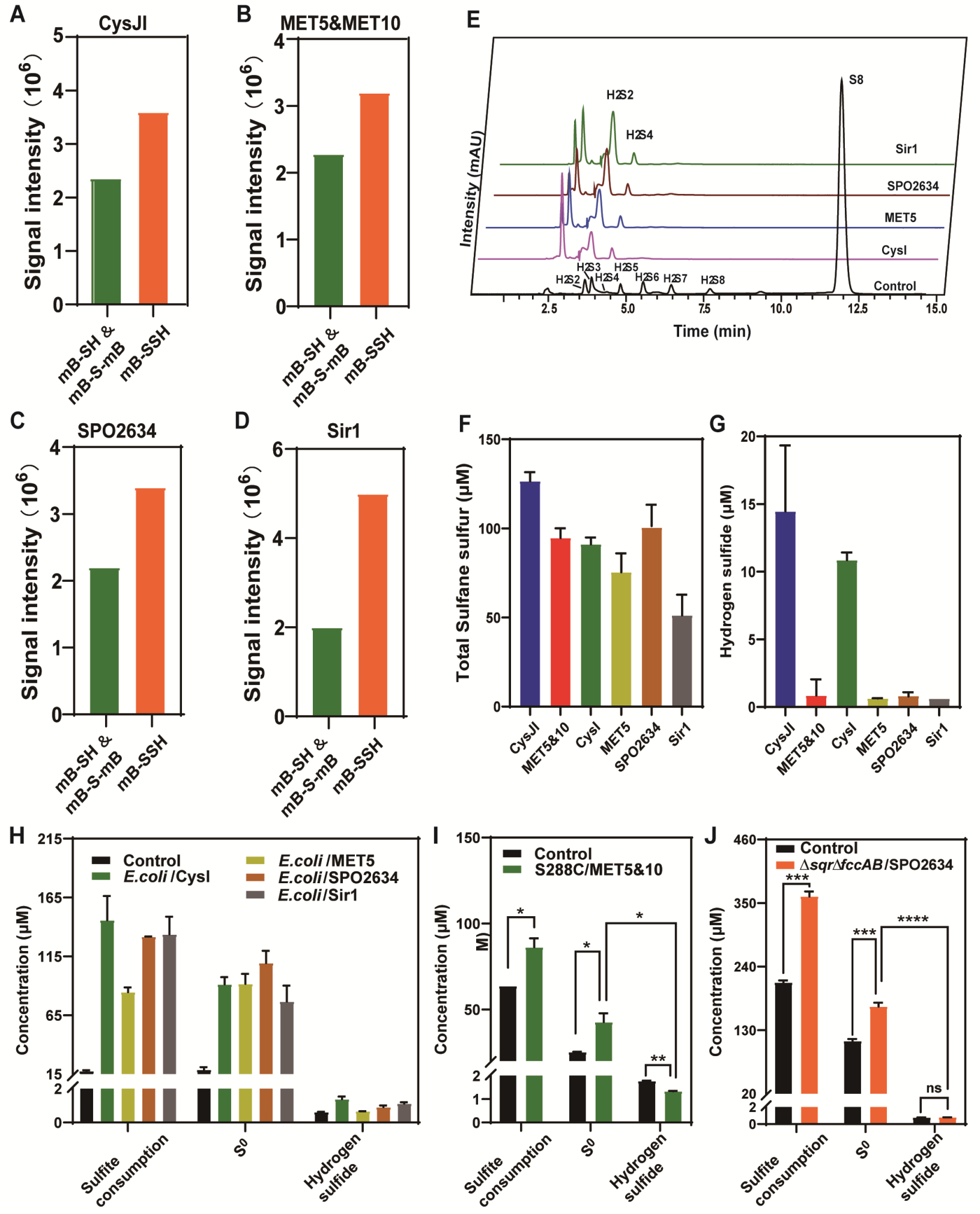
A
CysJI
Signal intensity (10^6)
mB-SH & mB-S-mB
mB-SSH
B
MET5&MET10
C
SPO2634
D
Sir1
E
Intensity (mAU)
Time (min)
S8
H2S2
H2S4
H2S3
H2S5
H2S6
H2S7
H2S8
Sir1
SPO2634
MET5
CysI
Control
F
Total Sulfane sulfur (μM)
CysJI
MET5&10
CysI
MET5
SPO2634
Sir1
G
Hydrogen sulfide (μM)
H
Control
E.coli /CysI
E.coli /MET5
E.coli /SPO2634
E.coli /Sir1
Concentration (μM)
Sulfite consumption
S0
Hydrogen sulfide
I
Control
S288C/MET5&10
J
Control
ΔsqrΔfccAB/SPO2634
ns

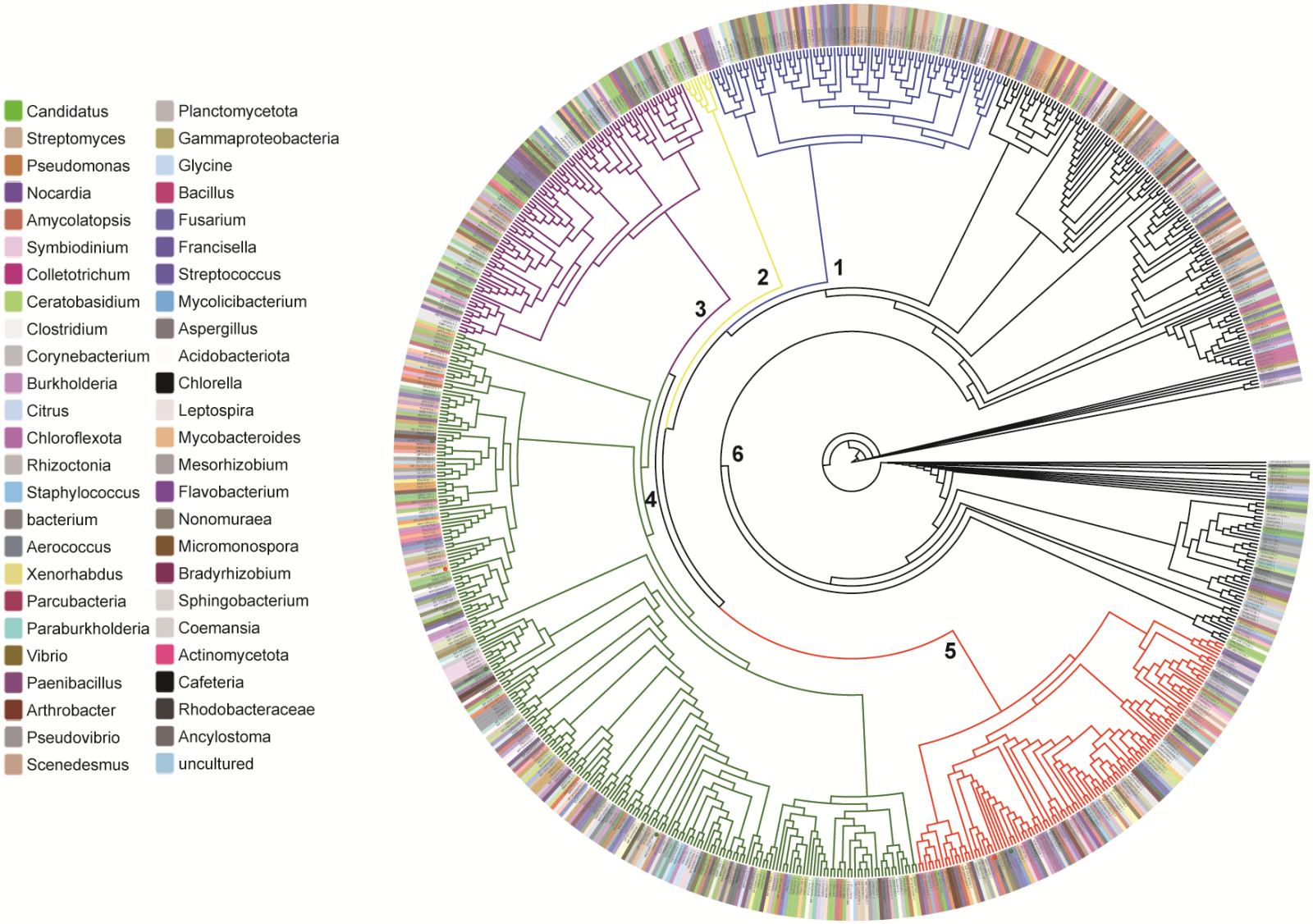
Candidatus
Streptomyces
Pseudomonas
Nocardia
Amycolatopsis
Symbiodinium
Colletotrichum
Ceratobasidium
Clostridium
Corynebacterium
Burkholderia
Citrus
Chloroflexota
Rhizoctonia
Staphylococcus
bacterium
Aerococcus
Xenorhabdus
Parcubacteria
Paraburkholderia
Vibrio
Paenibacillus
Arthrobacter
Pseudovibrio
Scenedesmus
Planctomycetota
Gammaproteobacteria
Glycine
Bacillus
Fusarium
Francisella
Streptococcus
Mycolicibacterium
Aspergillus
Acidobacteriota
Chlorella
Leptospira
Mycobacteroides
Mesorhizobium
Flavobacterium
Nonomuraea
Micromonospora
Bradyrhizobium
Sphingobacterium
Coemansia
Actinomycetota
Cafeteria
Rhodobacteraceae
Ancylostoma
uncultured
1
2
3
4
5
6

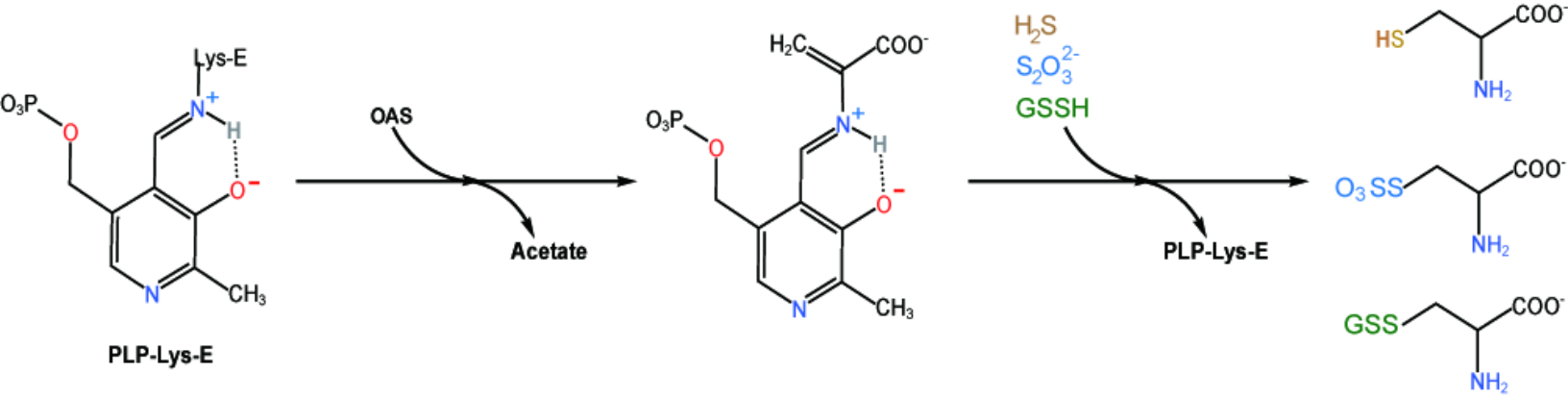
Lys-E
O3P
O
N+
H
O-
N
CH3
PLP-Lys-E
OAS
Acetate
H2C
COO-
O3P
O
N+
H
O-
N
CH3
H2S
S2O3 2-
GSSH
PLP-Lys-E
HS
COO-
NH2
O3SS
COO-
NH2
GSS
COO-
NH2

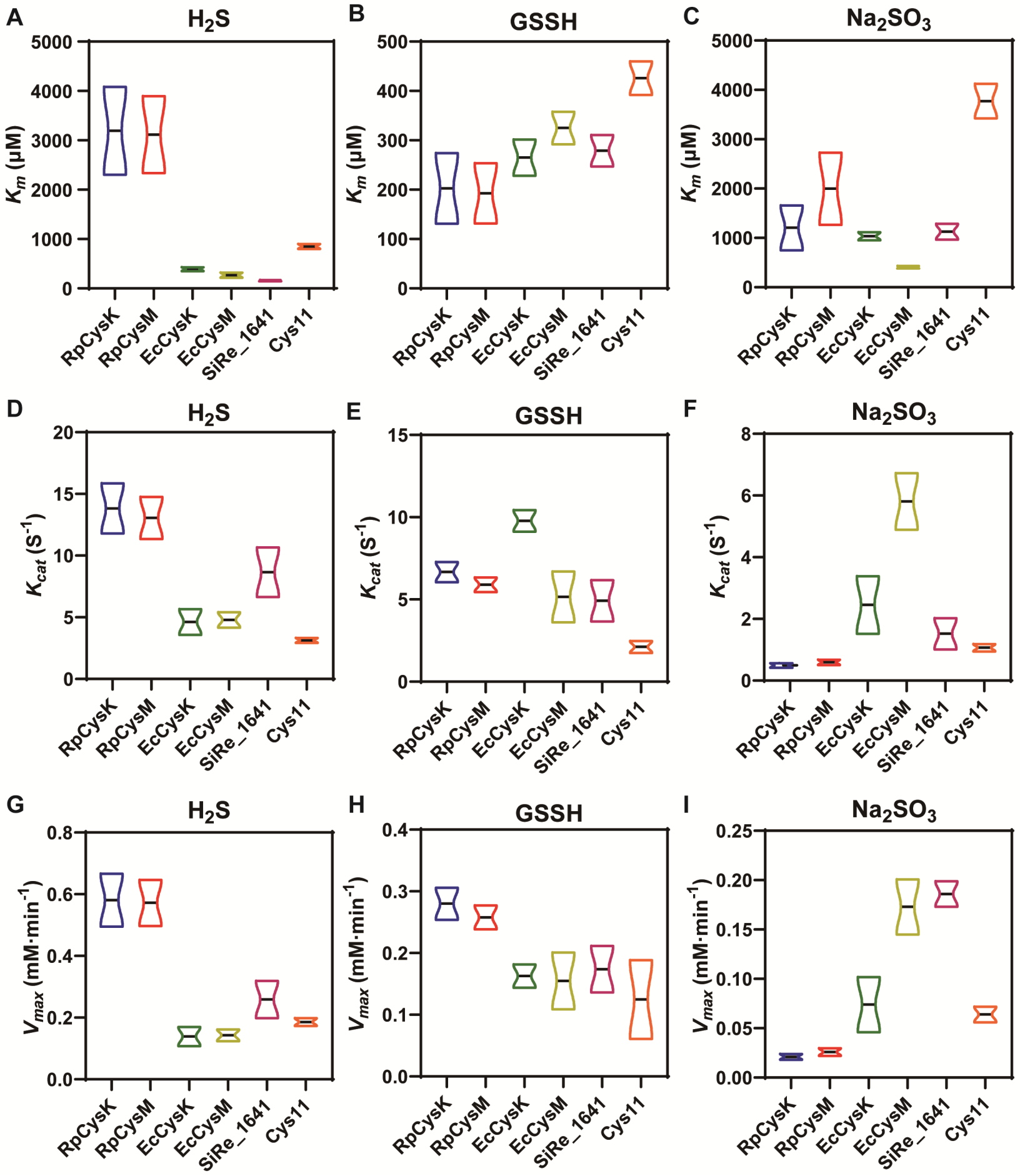
A
H2S
Km (μM)
5000
4000
3000
2000
1000
0
B
GSSH
Km (μM)
500
400
300
200
100
0
C
Na2SO3
Km (μM)
5000
4000
3000
2000
1000
0
D
H2S
Kcat (S-1)
20
15
10
5
0
E
GSSH
Kcat (S-1)
15
10
5
0
F
Na2SO3
Kcat (S-1)
8
6
4
2
0
G
H2S
Vmax (mM·min-1)
0.8
0.6
0.4
0.2
0.0
H
GSSH
Vmax (mM·min-1)
0.4
0.3
0.2
0.1
0.0
I
Na2SO3
Vmax (mM·min-1)
0.25
0.20
0.15
0.10
0.05
0.00
RpCysK
RpCysM
EcCysK
EcCysM
SiRe_1641
Cys11

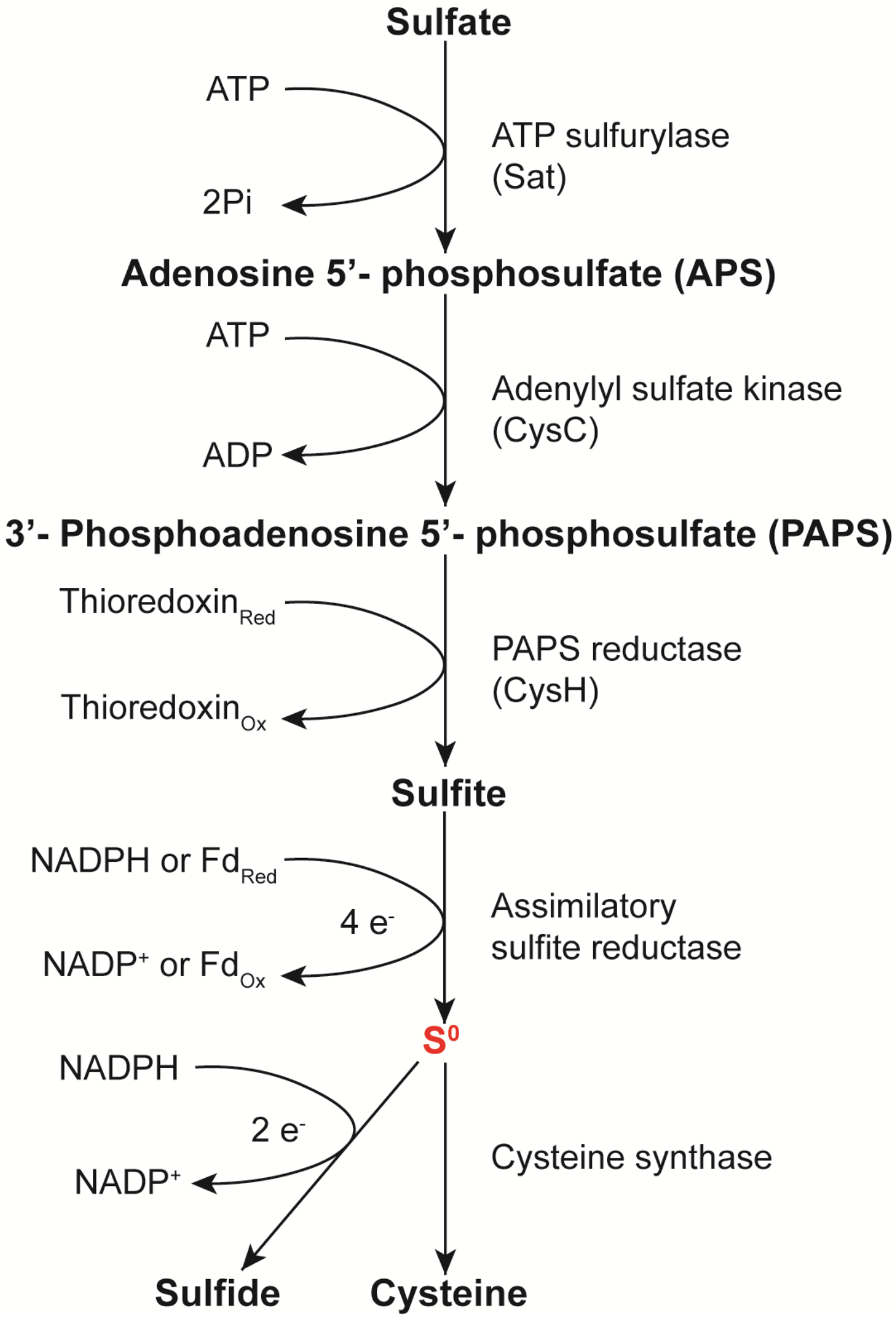
Sulfate
ATP
2Pi
ATP sulfurylase
(Sat)
Adenosine 5'- phosphosulfate (APS)
ATP
ADP
Adenylyl sulfate kinase
(CysC)
3'- Phosphoadenosine 5'- phosphosulfate (PAPS)
Thioredoxin Red
Thioredoxin Ox
PAPS reductase
(CysH)
Sulfite
NADPH or Fd Red
4 e-
NADP+ or Fd Ox
Assimilatory
sulfite reductase
S0
NADPH
2 e-
NADP+
Cysteine synthase
Sulfide
Cysteine